Anisotropic waveguides induced by photorefractive (2+1)D solitons

J. Petter

Institute of Applied Physics, Darmstadt University of Technology, Hochschulstrasse 6, D-64289 Darmstadt, Germany

C. Denz

Institut für Angewandte Physik, Westfälische Wilhelms-Universität, Correnstrasse 2/4, D-48149 Münster, Germany

A. Stepken and F. Kaiser

Institute of Applied Physics, Darmstadt University of Technology, Hochschulstrasse 4, D-64289 Darmstadt, Germany

Received June 20, 2001; revised manuscript received October 29, 2001

We present theoretical and experimental investigations of the anisotropic character of the refractive-index modulation that is induced by a light beam propagating in a photorefractive strontium barium niobate crystal. Such a structure creates a so-called spatial screening soliton that is able to carry a second wave of a different wavelength and therefore can act as a waveguide. We show in numerical simulations as well as in experimental investigations the anisotropic property of refractive-index modulation. Furthermore, the noncircular shape of the induced waveguide is justified by the excitation of higher-order modes, which were found to be asymmetric in both transverse directions. Whereas in the direction perpendicular to the applied electric field the TEM_{01} and TEM_{02} modes can easily be excited, excitement of the TEM_{10} mode in the direction of the applied field is rather difficult. This effect can be explained by the constricted extension of the waveguide in this direction.

OCIS codes: 190.0190, 190.4420, 230.7370.

1. INTRODUCTION

The topic of spatial optical solitons has been discussed thoroughly during the past decade. The effect of the balance between the natural divergence and the self-focusing of a light beam in a nonlinear optical material has attracted the interest of many scientists.[1–4] The stable propagation of spatially two-dimensional self-focused beams in saturable nonlinear materials[5] and especially in photorefractive (PR) media[6,7] affords a variety of possible applications. Besides the manifold of interactions between two or more of these so-called spatial solitons, the capability of the solitons to guide waves of different wavelengths provides a promising property for applications in all-optical information processing and optical switching and routing. These properties of spatial solitons were discussed extensively in several recent publications (e.g., Refs. 8–11).

Although self-focusing of optical beams and the formation of spatial solitons were described in a variety of media,[5,12,13] PR solitons are unique for various reasons. Spatial PR solitons emerge when light beams of appropriate wavelength, intensity, and shape are launched into a PR crystal and a dc electric field is applied in the lateral direction. The propagating light beams induce free charge carriers whose redistribution owing to drift and diffusion screens the externally applied field. The internal field changes the refractive index by means of the linear Pockels effect. The most important feature of PR crystals is the saturable character of the nonlinearity, which allows for self-trapping in one and two transverse dimensions at very low (a few microwatts) optical power levels. Another relevant difference from, e.g., Kerr-type solitons is the nonlocality and the anisotropic character of the medium's response to incident light beams, which is an inherent feature of the photorefractive material. Modulation of the refractive index is rather complex. Because of the orientation of the external electric field along one transverse direction and owing to the anisotropic crystal structure, self-focusing in PR crystals is anisotropic and therefore does not allow for circularly symmetric solutions.[14–16] Roughly speaking, the refractive index is increased in the area illuminated by the beam; in the adjoining regions the index is decreased along the direction of the external field and increased in the perpendicular direction. Whereas increasing the index allows for focusing, reducing the index leads to defocusing of the propagating beam.[17] Because of this structure two or more solitons may interact in a variety of ways that are not necessarily related to, e.g., solitons in quadratic media. These interactions, including attraction, repulsion, rotation, mutual oscillation, and exchange of energy even for incoherent beams, were subjects of close examination in several studies (see, e.g., Refs. 4, 18, and 19).

Such anisotropy was examined previously in PR $Bi_{20}Ti_{20}$ crystals. In that case an interferometric measurement technique was used to illustrate the phase dis-

tribution of the induced refractive-index profile.[20] However, here we focus on the anisotropy of self-focusing in PR $Sr_{0.60}Ba_{0.40}Nb_2O_6$ (SBN60:Ce; SBN) crystals, where we can show the difference between focusing in the two transverse dimensions by scanning the structure directly with a probe beam. The investigations were made in experiments as well as in numerical simulations, and we found good agreement between experimental and numerical data. Additionally, we proved the anisotropic noncircular shape of the induced refractive-index modulation by using the waveguide characteristics of these structures. When a nonerasing probe beam was coupled into such a waveguide, which was slightly shifted to the center of the beam, we were able to excite higher-order transverse modes of this waveguide. Whereas the TEM_{01} and TEM_{02} modes could be excited easily, excitation of the TEM_{10} mode in the direction of the applied electric field was almost impossible. Again, these experimental results are in accordance with the numerical simulations.

2. THEORETICAL MODEL

In contrast to that of Kerr-type media, the response of PR crystals is wavelength dependent. In the band-transport model of Kukhtarev *et al.*[21] the redistributed charges come from the donator levels. In this picture, only light within a certain, relatively small spectral range is assumed to be able to modulate the refractive indices of PR crystals. As a consequence, one can generate waveguiding structures inside the PR crystal. However, these waveguides can guide beams of wavelengths at which the material is less photosensitive. Because they have different wavelengths, these beams possess different focusing and defocusing properties.

In general, the propagation of optical beams inside a PR crystal can be described by a standard wave equation in the paraxial approximation.[22] First, we model the generation of solitons inside the SBN crystal. A laser beam with $\lambda = 532$ nm wavelength is well suited to modify the refractive index. The propagation of the slowly varying envelope $A(x, y)$ is described by the paraxial propagation equation

$$\partial_z A - 1/2i\nabla^2 A + 1/2i\gamma(\partial_x \phi - E_0)A = 0, \qquad (1)$$

where $\gamma = n_0^4 r k_0^2 w_0^2$ is the photorefractive coupling constant with vacuum wave vector k_0, $n_0 = 2.35$ is the unperturbed refractive index, the dominant electro-optic coefficient of SBN at $\lambda = 532$ nm is $r_{33} = 1.8 \times 10^{-8}$ cm/V, and the w_0 is transverse scaling. E_0 is the strength of the externally applied field, and ϕ is the electrostatic potential induced by the light, whose spatial evolution is described by the following potential equation[23]:

$$\Delta\phi + \nabla \ln(1 + I)\nabla\phi = E_0 \partial_x \ln(1 + I) - \frac{k_B T}{e}[\nabla^2 \ln(1 + I) + (\nabla \ln(1 + I))^2], \qquad (2)$$

where $I = |A|^2$ is the transverse intensity distribution normalized to saturation intensity I_d, k_B is Boltzmann's constant, and T is the temperature.

For optical guiding we use a second laser beam with a slowly varying amplitude $B(x, y)$ and a different wavelength. It is assumed that this beam does not alter the refractive-index distribution, which is hence just a function of the soliton beam: $\phi = \phi(A)$. The propagation of the probe beam is described by the modified paraxial propagation equation

$$\partial_z B - \frac{1}{2} i \frac{\lambda'}{\lambda} \nabla^2 B + \frac{1}{2} i \frac{\lambda r'}{\lambda' r} \gamma(\partial_x \phi - E_0)B = 0, \qquad (3)$$

where $r' = 1.2 \times 10^{-8}$ cm/V is the electro-optic coefficient in SBN for beams with a wavelength of $\lambda' = 633$ nm. The frequency dependence of the unperturbed refractive index n_0 is neglected: $n_0(\lambda) \approx n_0(\lambda')$. Compared with the soliton beam, the probe beam diffracts and focuses in a different way, which is reflected by the additional terms in Eq. (3).

The propagation equations are solved by a modified beam-propagation method,[24] and the potential equation is treated by the Crank–Nicholson finite-difference scheme.

3. EXPERIMENTAL REALIZATION

The experimental examination of the anisotropic refractive-index modulation was done with a standard configuration.[25] A laser beam was derived from a frequency-doubled Nd:YAG laser ($\lambda = 532$ nm, $I \approx 850$ mW/cm^2) and focused to a size of nearly 20 μm (FWHM) onto the front face of the SBN crystal. The crystal was doped with 0.002 wt% CeO_2, and its dimensions were 5 mm × 5 mm × 20 mm. An electric dc field, $E_0 = 1.8$ kV/cm, was applied along the crystallographic c axis. To exploit the dominant electro-optic coefficient r_{33} of SBN, we linearly polarized the propagating light parallel to the c axis. The back face of the crystal was monitored with a CCD camera.

The light-induced screening of an applied electric field is determined by the degree of saturation of the photorefractive nonlinearity, which is proportional to the ratio between the soliton peak intensity and the background illumination. To control the level of saturation, we illuminated the crystal with a wide beam provided by an incoherent white-light source. In this way we were able to form a two-dimensional, elliptically shaped steady-state screening soliton.[26]

To gain further insight into the nonlocal character of the refractive-index distribution in the transverse plane we expanded the setup to scan the region about the propagating beam. We did so by using the broad beam of a He–Ne laser with $\lambda = 633$ nm propagating along the path of the previously written waveguide (Fig. 1). Be-

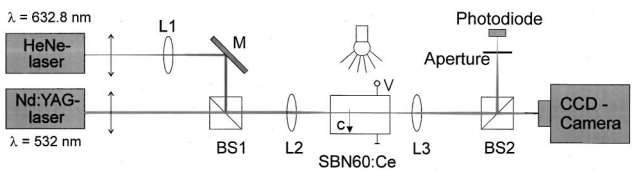

Fig. 1. Schematic of setup for examining the structure of induced waveguides. Beam splitter BS2 and the photodiode are used only for measuring the guiding capability of the structure. L1–L3, lenses; M, mirror; BS1, beam splitter.

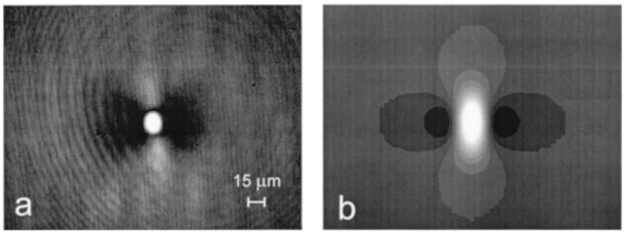

Fig. 2. a, Back face of the crystal when the waveguide, which previously was induced by a green writing beam, is scanned with the broadened red probe beam. b, Contour plot of the refractive-index modulation obtained by numerical simulation. In both a and b the dark defocusing areas on both sides of the central part of the structure exist only in the x direction (direction of the externally applied electric field).

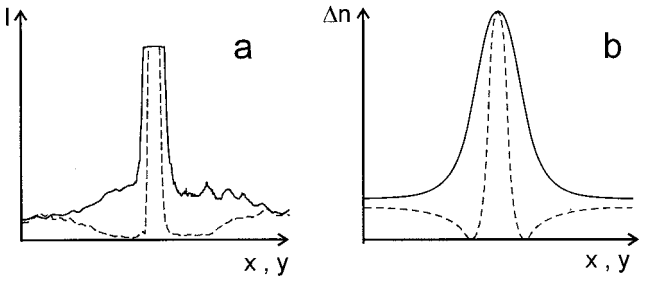

Fig. 3. x and y cuts through a, the intensity distribution in experiment and b, the modulation of the refractive index in the numerical simulation. Dashed curves, cuts along the x direction; solid curves along the y direction. The flattened tip of the curve in a is due to overexposure by the camera.

cause of the low dark conductivity of our crystal we found that the induced refractive-index change was present for a long time after we switched off the writing beam and the background illumination. Hence we were able to scan the previously written structure with the red probe beam. Moreover, the PR material is less sensitive to light in the red wavelength region, and therefore the induced refractive-index modulation could be scanned without actually being erased. By shifting the focusing lens in front of the crystal we set the diameter of the red probe beam to be approximately seven times larger (diameter, $\approx$150 μm FWHM) than the diameter of the soliton beam. To reduce the possible influence of the probe beam on the waveguide, we set the intensity of the probe beam to $I \approx 8\ \mathrm{mW/cm^2}$.

Figure 2a shows the back face of the crystal when the probe beam is launched into the crystal and guided in a waveguide that had previously been induced by the writing beam. The central bright spot clearly shows that the main part of the probe beam's intensity is located close to the core of the waveguide. Around the center of the beam a widespread patch of light can be seen. This stems from light that is not coupled into the waveguide but has followed the natural divergence of the beam.

However, the two elliptical dark regions located close to the central spot are of more interest. As the refractive index is decreased in the regions close to the writing beam's center only along the direction of the externally applied field, the dark regions reflect the strong nonlocality and anisotropy of the index modulation.

The width of these defocusing areas, which is $\sim$30 μm to both sides of the beam, gives further evidence of the far-reaching modulation of the refractive index, which stems from the modulated electrostatic potential in the crystal. Comparing experimental examinations with numerically calculated index distributions yields good agreement. Figure 2b shows a contour plot of the refractive-index modulation induced by a single beam. Figure 3 compares the distribution of light intensity in experiment (Fig. 3a) and the modulation of the refractive index in numerical simulation (Fig. 3b) along the two perpendicular directions.

Taking into account the complex anisotropic structure, we can explain many interesting interaction models of two or more PR solitons. So the anomalous interaction of two solitons in the plane of the applied electric field is a consequence of the overlapping defocusing lobes. In the direction perpendicular to the external field there are no defocusing areas and therefore there is no repulsion between two solitons.[18] The interaction is Kerr-like, but, because of the nonlocal modulation of the index, attraction is possible even if the optical fields do not overlap.

4. EXCITATION OF TRANSVERSE MODES

Another evidence of the anisotropic nature of the induced waveguide is given by the excitation of transverse higher-order modes. Here pronounced differences between the two transverse directions can be found.

Whereas it was previously indicated that waveguides induced in PR SBN crystals have a rather circular shape and that transverse higher-order modes can be excited independently of their orientation,[9] we found large directional differences in the possibility of exciting these modes.

As both the numerically calculated and the experimentally scanned refractive-index distributions show, the waveguide is constricted along the direction of the external field and extended in the direction perpendicular to it, compared with a circularly symmetric writing beam.

In general, the waveguiding properties of refractive-index structures can be estimated by use of a dimensionless waveguide parameter W,[27] that is proportional to the diameter and the refractive index differences of the waveguide:

$$W \sim a\sqrt{n_+ - n_-}, \tag{4}$$

where a is the diameter and n_+ and n_- are the maximum and minimum values, respectively, of the refractive index. It is obvious that an anisotropic waveguide may carry higher-order modes preferably in the direction of its broader extension rather than in the other direction, because its guiding properties are linearly dependent on the diameter of the induced focusing refractive-index structures.

Experimental investigations were made in the same setup as for the scanning experiments explained above. This time the intensity of the green beam that was writing the waveguide was $I_{\mathrm{green}} \approx 55\ \mathrm{mW/cm^2}$, whereas the red probe beam had an intensity of $I_{\mathrm{red}} \approx 39\ \mathrm{mW/cm^2}$. The applied electric field was set to $E_0 = 1.8\ \mathrm{kV/cm}$. To achieve the best guiding characteristics in the core of the waveguide requires a high gradient of the refractive index. For this reason no background illumination was

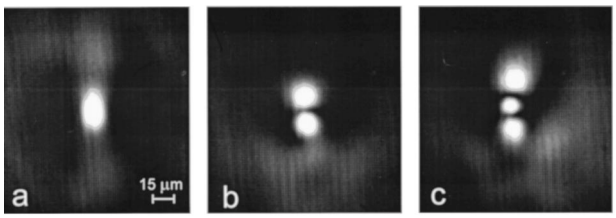

Fig. 4. Excitation of higher-order waveguide modes with the red probe beam in experiment: a, TEM_{00} mode; b, c, the first and second higher-order modes, TEM_{01} and TEM_{02}, respectively.

present during the writing process, which was stopped once the waveguide had formed.

To investigate the guiding properties of this waveguide we focused the red probe beam in a first experiment to the same size as the center of the waveguide (diameter $d \approx 20\,\mu$m) and found that more than 56% of its energy was guided in the core of the waveguide. This value includes all losses that stem from coupling the beam in and out of the crystal and is equivalent to a damping of $D = 2.46$ dB.

To excite higher-order modes of this waveguide, we broadened the red probe beam to a size $d \approx 100\,\mu$m at the front face of the crystal. Figure 4a shows the intensity distribution at the back side of the crystal when the red probe beam is launched coaxially into the waveguide. In this case only the zero-order (TEM_{00}) mode of the waveguide is excited. Note the elliptical shape of the guided beam and the dark (defocusing) areas near the beam scanned by light that was not coupled into the waveguide itself but scattered at its borders. The diameters must not coincide, because the guided beam diffracts and focuses in a slightly different way from the writing soliton. As a consequence, the zero order (TEM_{00}) of the guided beam will oscillate during propagation and will experience changes in its beam shape.

Higher-order modes are excited if the probe beam is shifted a few micrometers in one transverse direction with respect to the center of the previously written waveguide structure. In contrast to other investigations in which a dipole was launched into the waveguide,[9] we excited higher-order modes by launching a slightly shifted beam of Gaussian shape, as suggested in Ref. 28. When the probe beam was shifted in the y direction (perpendicular to the applied electric field) on the front face of the crystal, only a part of its spatially distributed intensity was coupled into the waveguide structure. This coupled intensity selects a certain range of the beam's spatial k-vectors, and the focused part of the beam inside the waveguide propagates nonparaxially. The same effect could be achieved if the probe beam were not shifted but were tilted with respect to the waveguide during coupling in.

By shifting the probe beam in the y direction ($\Delta y \approx 15\,\mu$m with respect the center of the waveguide) we were able to excite the higher-order (TEM_{01}) mode [Fig. 4b]. The same structure appeared when the beam was shifted the same distance in the opposite direction ($\Delta y \approx -15\,\mu$m). Shifting the probe beam for another 15 μm (total displacement, $\Delta y \approx 30\,\mu$m from the center of the waveguide) excited even the next-higher-order mode (TEM_{02}; see Fig. 4c).

These experimentally found data confirm the numerical results in an excellent way. In the simulations the parameters of the Gaussian beam writing the waveguide and the Gaussian probe beam were chosen to have a maximum intensity of $I_0 = 3$ (in units of I_d) and a diameter of $w = 15\,\mu$m. The strength of the external electric field was $E_0 = 2.5$ kV/cm.

Figure 5 shows the transverse intensity distributions of the probe beam leaving the crystal after propagation of length $z = 13.5$ mm. The three parts of the figure correspond to three different initial transversal displacements between probe beam and waveguide.

In snapshot a of Fig. 5 the probe beam is not shifted. With respect to the center of the waveguide, the probe beam focuses symmetrically. The initially circularly symmetric Gaussian beam couples into the anisotropic waveguide and gets an elliptical shape.

As soon as the probe beam is shifted, focusing of the beam becomes asymmetric with respect to the center of the waveguide. Spatial parts closer to the center focus more strongly than the other parts. However, because of the nonlocality of the waveguide, almost the entire probe beam remains focused if it is displaced along the y direction. If the probe beam is shifted by $\Delta y = 15\,\mu$m, as shown in Fig. 5b, a TEM_{01} mode is excited and the probe beam propagates in the form of a dipole. Second-order mode TEM_{02} appears if the displacement between waveguide and probe beam is increased to $\Delta y = 30\,\mu$m.

When the probe beam is shifted along the direction of the externally applied electric field, it turns out to be difficult to excite higher modes experimentally. We were not able even to realize TEM_{10} modes. In Figs. 6a and 6b two examples are shown, displacements of $\Delta x = \pm 15\,\mu$m. Obviously, the shift between the center of the probe beam and the center of the waveguide is too large, and most of the probe beam defocuses in the regions of reduced refractive index. The pronounced difference between the two transverse directions clearly demonstrates the anisotropic character of the induced refractive-index structure.

However, numerical simulations show that it should be possible to excite higher-order modes along the direction of the external field. By adjusting the parameter carefully in the simulation we were able to excite the TEM_{10} mode also, as shown in Fig. 6c. To obtain these results we broadened the diameter of the writing beam to $\approx 50\,\mu$m, which was not possible in experiment because inhomogeneities of the material led to immediate filamentation. Nevertheless, in Fig. 6c the smaller extension of the modal structure along this direction is obvious.

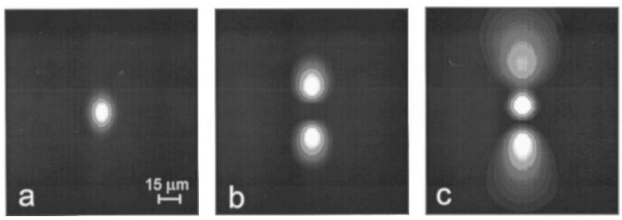

Fig. 5. Excitation of the higher-order waveguide modes with the red probe beam in numerical simulation: a, TEM_{00} mode; b, c, first and second higher-order modes, TEM_{01} and TEM_{02}, respectively.

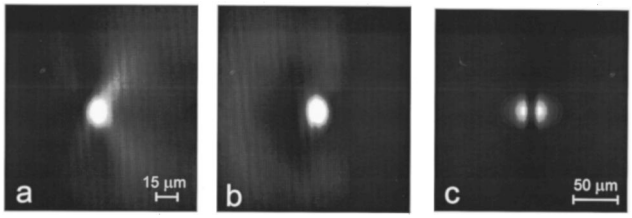

Fig. 6. a, b, Excitation of the first higher-order TEM_{10} modes in the x direction is not possible in experiment. c, In the numerical simulation the excitation of the TEM_{10} mode is possible only in a very broad waveguide.

5. CONCLUSION

Photorefractive spatial solitons are known for their properties of guiding waves of different wavelengths. Their easy creation and their stability make them interesting candidates for applications in all-optical information processing, guiding, and routing of optical signals. The unexpected interaction between two or more of them may enhance the list of possible applications. However, this manifold of interaction models is due to the anisotropic character of the induced refractive-index modulation. So, when thinking of the implementation of photorefractive solitons in signal processing devices, one always has to take into account this anisotropy. Here we showed two different ways to illustrate the anisotropic shape of the induced waveguide. In a scanning experiment the different areas of focusing and defocusing are shown; in another experiment we found a pronounced difference between the excitation of higher-order modes in the two transverse dimensions. In both cases the data of the numerical simulations were found to be in good accordance with the experimental results.

ACKNOWLEDGMENTS

J. Petter and C. Denz acknowledge the kind support of T. Tschudi. J. Petter's e-mail address is juergen.petter @physik.tu-darmstadt.de.

REFERENCES

1. M. Segev, "Optical spatial solitons," Opt. Quantum Electron. **30**, 503–533 (1998).
2. M. Mitchell, M. Segev, T. H. Coskun, and D. N. Christodoulides, "Theory of self-trapped spatially incoherent light beams," Phys. Rev. Lett. **79**, 4990–4993 (1997).
3. H. Meng, G. Salamo, and M. Segev, "Primarily isotropic nature of photorefractive screening solitons and the interactions between them," Opt. Lett. **23**, 897–899 (1998).
4. W. Krolikowski, M. Saffman, B. Luther-Davies, and C. Denz, "Anomalous interaction of spatial solitons in photorefractive media," Phys. Rev. Lett. **80**, 3240–3243 (1998).
5. J. E. Bjorkholm and A. Ashkin, "CW self-focusing and self-trapping of light in sodium vapor," Phys. Rev. Lett. **32**, 129–132 (1974).
6. M. Segev, B. Crosignani, A. Yariv, and B. Fischer, "Spatial solitons in photorefractive media," Phys. Rev. Lett. **68**, 923–926 (1992).
7. G. Duree, J. L. Shultz, G. Salamo, M. Segev, A. Yariv, B. Crosignani, P. DiPorto, E. Sharp, and R. Neurgaonkar, "Observation of self-trapping of an optical beam due to the photorefractive effect," Phys. Rev. Lett. **71**, 533–536 (1993).
8. Z. Chen, M. Segev, D. N. Christodoulides, and R. S. Feigelson, "Waveguides formed by incoherent dark solitons," Opt. Lett. **24**, 1160–1162 (1999).
9. M. Shih, M. Segev, and G. Salamo, "Circular waveguides induced by two-dimensional bright steady-state photorefractive spatial screening solitons," Opt. Lett. **21**, 931–933 (1996).
10. M. Shih, Z. Chen, M. Mitchell, M. Segev, H. Lee, R. Feigelson, and J. P. Wilde, "Waveguides induced by photorefractive screening solitons," J. Opt. Soc. Am. B **14**, 3091–3101 (1997).
11. J. Petter and C. Denz, "Guiding and dividing waves with photorefractive solitons," Opt. Commun. **188**, 55–61 (2001).
12. A. Barthelemy, S. Maneuf, and C. Froehly, "Propagation soliton et auto-confinement de faisceaux laser par non linearite optique de Kerr," Opt. Commun. **55**, 201–206 (1985).
13. J. S. Aitchison, A. M. Weiner, Y. Silberberg, M. K. Oliver, J. L. Jackel, D. E. Leaird, E. M. Vogel, and P. W. E. Smith, "Observation of spatial optical solitons in a nonlinear glass waveguide," Opt. Lett. **15**, 471–473 (1990).
14. A. A. Zozulya, D. Z. Anderson, A. V. Mamaev, and M. Saffman, "Solitary attractors and low-order filamentation in anisotropic self-focusing media," Phys. Rev. A **57**, 522–534 (1998).
15. S. Gatz and J. Herrmann, "Anisotropy, nonlocality, and space-charge field displacement in (2+1)-dimensional self-trapping in biased photorefractive crystals," Opt. Lett. **23**, 1176–1178 (1998).
16. M. Saffman and A. A. Zozulya, "Circular solitons do not exist in photorefractive media," Opt. Lett. **23**, 1579–1581 (1998).
17. A. A. Zozulya and D. Z. Anderson, "Propagation of an optical beam in a photorefractive medium in the presence of a photogalvanic nonlinearity or an externally applied electric field," Phys. Rev. A **51**, 1520–1531 (1995).
18. W. Krolikowski, B. Luther-Davies, C. Denz, J. Petter, C. Weilnau, A. Stepken, and M. R. Belic, "Interaction of two-dimensional spatial incoherent solitons in photorefractive medium," Appl. Phys. B **68**, 975–982 (1999).
19. C. Denz, W. Krolikowski, J. Petter, C. Weilnau, T. Tschudi, M. R. Belic, F. Kaiser, and A. Stepken, "Dynamics of formation and interaction of photorefractive screening solitons," Phys. Rev. E **60**, 6222–6225 (1999).
20. G. S. G. Quirino, M. D. I. Castillo, J. J. Sánchez-Mondragón, S. Stepanov, and V. Vysloukh, "Interferometric measurements of the photoinduced refractive index profiles in photorefractive $Bi_{12}TiO_{20}$ crystal," Opt. Commun. **123**, 597–602 (1996).
21. N. V. Kukhtarev, V. B. Markov, S. G. Odulov, M. S. Soskin, and V. L. Vinetskii, "Holographic storage in electrooptic crystals. I. Steady state; II. Beam coupling–light amplification," Ferroelectrics **22**, 949–964 (1979).
22. A. W. Snyder and Y. S. Kivshar, "Bright spatial solitons in non-Kerr media: stationary beams and dynamical evolution," J. Opt. Soc. Am. B **14**, 3025–3031 (1997).
23. A. Stepken, F. Kaiser, and M. R. Belic, "Anisotropic interaction of three-dimensional spatial screening solitons," J. Opt. Soc. Am. B **17**, 68–77 (2000).
24. M. Lax, G. P. Agrawal, M. R. Belic, B. J. Coffey, and W. L. Louisell, "Electromagnetic-field distributions in loaded unstable resonators," J. Opt. Soc. Am. A **2**, 731–742 (1985).
25. J. Petter, C. Weilnau, C. Denz, A. Stepken, and F. Kaiser, "Self-bending of photorefractive solitons," Opt. Commun. **170**, 291–297 (1999).
26. A. A. Zozulya, D. Z. Anderson, A. V. Mamaev, and M. Saffman, "Self-focusing and soliton formation in media with anisotropic nonlocal material response," Europhys. Lett. **36**, 419–424 (1996).
27. A. W. Snyder, D. J. Mitchell, and Y. S. Kivshar, "Unification of linear and nonlinear wave optics," Mod. Phys. Lett. B **9**, 1479–1506 (1995).
28. N. S. Kapany and J. J. Burke, *Optical Waveguides* (Academic, New York, 1972).